

**Role of the apical oxygen in the low-temperature magnetoelectric effect in  $RMnO_3$  ( $R = Ho$  and  $Lu$ )**

J. Vermette and S. Jandl

*Département de Physique, Université de Sherbrooke, 2500 Boulevard Université, Sherbrooke, Canada J1K 2R1*

M. Orlita

*Grenoble High Magnetic Field Laboratory, 25 Avenue des Martyres, Boîte Postale 166, F-38042 Grenoble, France*

M. M. Gospodinov

*Institute of Solid State Physics, Bulgarian Academy of Sciences, 1784 Sofia, Bulgaria*

(Received 26 October 2011; published 25 April 2012)

Infrared active phonons of  $HoMnO_3$  and  $LuMnO_3$  single crystals are studied under an applied magnetic field below  $Ho^{3+}$  spin ordering at  $T = 4.2$  K. Interestingly, relatively strong mode energy shifts, induced by the magnetic field, are observed in  $HoMnO_3$  but are absent in the nonmagnetic rare-earth compound  $LuMnO_3$ . We associate the large magnetoelectric effects in  $HoMnO_3$  with a mechanism of charge transfer between  $Ho^{3+}$  and apical oxygen. Also, the exact values of the published polarization change under the applied magnetic field are predicted with no adjustable parameters.

DOI: [10.1103/PhysRevB.85.134445](https://doi.org/10.1103/PhysRevB.85.134445)

PACS number(s): 75.85.+t, 75.30.Et, 78.30.Er

**I. INTRODUCTION**

Multiferroic materials are promising candidates for new innovative devices, particularly in the field of memory storage.<sup>1</sup> The strong coupling between magnetic ordering and ferroelectricity characterizing these compounds allows the modulation of the electric polarization (magnetic moment) with an external magnetic (electric) field.<sup>2,3</sup> The origin of ferroelectricity, which is different depending on the multiferroic compound, results in a variety of magnetoelectric coupling strengths. In orthorhombic type-II multiferroics ( $Tb$ ,  $Dy$ ) $MnO_3$  and ( $Nd$ ,  $Tb$ ,  $Dy$ ) $Mn_2O_5$ , ferroelectricity is directly induced by a commensurate spiral magnetic ordering via Dzyaloshinskii-Moriya interaction giving a strong magnetoelectric coupling with a relative small polarization of  $\sim 10^{-2} \mu C cm^{-2}$ .<sup>3,4</sup> Hexagonal  $RMnO_3$  ( $R = Ho$  to  $Lu$ ) compounds are type-I multiferroics in which ferroelectricity and magnetism have different sources giving a relative weak magnetoelectric coupling with a large polarization of  $\sim 1 \mu C cm^{-2}$ . In this latter case ferroelectricity is induced at a relatively high temperature ( $T_C \sim 800$  K) following a structural transition to a noncentrosymmetric  $P6_3cm$  space group while magnetic ordering of  $Mn^{3+}$  and  $R^{3+}$  occurs at lower temperatures ( $T < 100$  K).  $Mn^{3+}$  spin frustration develops with an unusually large atomic displacement of rare-earth ions in the  $c$ -axis direction and of manganese ions in the  $ab$  plane.<sup>5</sup> Magnetoelectric coupling has been particularly retraced through the dielectric constant temperature dependence anomalies at the magnetic transitions.<sup>6</sup> In addition, strong spin-lattice interactions in the hexagonal  $RMnO_3$  have been observed with Raman spectroscopy<sup>7,8</sup> and infrared reflectance.<sup>9-11</sup> Remarkably, a giant flexoelectric effect has been reported in  $HoMnO_3$ , thus reflecting the oxygen role in the electric polarization strain gradient modulation.<sup>12</sup> Superexchange interaction between manganese and rare-earth ions is expected to play an important role in the magnetoelectric coupling.<sup>8,13,14</sup> Exchange striction has also been invoked near the Néel temperature in  $YMnO_3$  to explain the variations of the Mn-O bond lengths and O-Mn-O

bond angles and their modifications in the presence of a magnetic field.<sup>15</sup> More recently, the mechanism of charge transfer seems to play a role in the ferroelectric properties of hexagonal  $RMnO_3$ .<sup>11,16-20</sup> However, the mechanism of low-temperature magnetoelectric effect in this class of material is still in need of clarification.  $HoMnO_3$  and  $LuMnO_3$  are prototypes of hexagonal  $RMnO_3$  that crystallize in the  $P6_3cm$  space group. Their structures are formed by corner-sharing trigonal  $MnO_5$  bipyramids separated by layers of rare-earth ( $R$ ) ions located at  $C_{3v}$  ( $R_1$ ) and  $C_3$  ( $R_2$ ) points of symmetry.<sup>9</sup>  $HoMnO_3$  exhibits ferroelectric ordering along the  $c$  axis at  $T_{FE} \sim 875$  K resulting in two nonequivalent rare-earth sites  $R_1$  and  $R_2$  (Fig. 1). The symmetry of its  $Mn^{3+}$  antiferromagnetic phase transition (magnetic space group  $P6'_3c'm$ ) at  $T_N \sim 72$  K and its  $90^\circ$  in-plane spin reorientation at  $T_{SR} \sim 38$  K ( $P6'_3cm'$ ) has been resolved by second harmonic generation.<sup>21</sup> On the other hand,  $Mn^{3+}$  antiferromagnetic phase transition in  $LuMnO_3$  occurs at  $T_N \sim 90$  K and its spin reorientation at  $T_{SR}$  occurs approximately between 20 and 30 K.<sup>21,22</sup> For both crystals, previous studies have indicated that the temperature dependence of reflectance spectra show no structural transition except some phonon energy shifts.<sup>10,22</sup> Particular attention was focused on the  $E1$   $247 cm^{-1}$  mode energy shift of  $HoMnO_3$  as a function of temperature given its important extra hardening at the Néel transition. This behavior has been associated with spin-phonon coupling that involves basal oxygens and magnetic frustration.<sup>10</sup> Similar extra hardenings have been observed in Raman-active phonons of the hexagonal manganite family.<sup>7,8,10</sup> The combination of second harmonic generation with the Faraday rotation technique has particularly established an anisotropic superexchange magnetic interaction between the  $Mn^{3+}$  planes through the rare-earth ions.<sup>13</sup> Remarkably, the magnetic ordering in  $HoMnO_3$  is switchable from  $Ho^{3+}$  paramagnetic to  $Ho^{3+}$  ferromagnetic with an applied electric field. The driving mechanism being associated with an interplay of  $Ho^{3+}$ - $Mn^{3+}$  interaction and ferroelectric distortion.<sup>2</sup> A recent study of  $HoMnO_3$  atomic parameters refined from neutron powder-diffraction experiments at 40 K

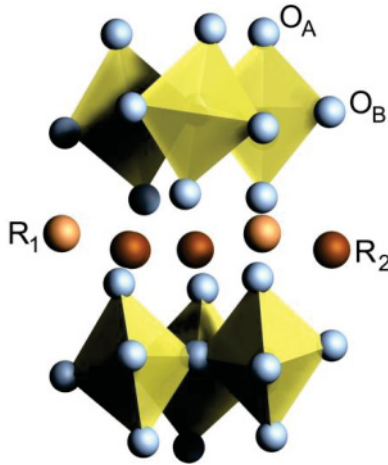


FIG. 1. (Color online) View of the tilted hexahedral cages sharing the basal oxygen ( $O_B$ ) in the  $ab$  plane.  $O_A$  corresponds to apical oxygen while manganese ions are located inside the cages.

( $P6_3c'm$ ) has shown that the vertical shift of the rare-earth  $\text{Ho}^{3+}$  ions is responsible for the ferroelectricity and for the important changes in the polarization as a function of temperature.<sup>3</sup> Upon cooling below  $T_{SR}$  ( $P6_3cm'$ ) the exchange interaction between  $\text{Ho}^{3+}$  and  $\text{Mn}^{3+}$  provokes ordering of the  $\text{Ho}_1$  and  $\text{Ho}_2$  moments along the  $c$  axis with a ferrimagnetic alignment in the  $ab$  plane; concomitantly the polarization decreases abruptly. Below  $T_{\text{Ho}} \sim 5$  K ( $P6_3cm$ ), the  $\text{Ho}_2$  moments order antiferromagnetically in the  $ab$  plane while the  $\text{Ho}_1$  moments become paramagnetic and the electric polarization is radically enhanced.

In order to determine which atoms play a major role in the low-temperature magnetoelectric effect, we study the evolutions of infrared active phonon frequencies (TO and LO) in  $\text{HoMnO}_3$  and  $\text{LuMnO}_3$  under an applied magnetic field below  $T_{\text{Ho}}$ . By comparing the renormalized force constants and the Born effective charges, the role of apical oxygen ( $O_A$ )<sup>7</sup> in  $\text{Ho}^{3+}$ - $\text{Mn}^{3+}$  superexchange interaction is particularly underlined.

## II. EXPERIMENT

Pure polycrystalline hexagonal  $\text{RMnO}_3$  ( $R = \text{Ho}$  and  $\text{Lu}$ ) was synthesized by a solid-state reaction of stoichiometric amounts of  $\text{R}_2\text{O}_3$  (99.99%) and  $\text{MnO}_2$  (99.99%) and annealed for 24 h at 1120 °C in an oxygen atmosphere.  $\text{RMnO}_3$  single crystals were grown by a high-temperature solution growth method using  $\text{PbF}_2/\text{PbO}/\text{B}_2\text{O}_3$  flux ( $\text{PbF}_2 : \text{PbO} : \text{B}_2\text{O}_3 = 0.8 : 0.195 : 0.005$ ). Flux was mixed with the  $\text{RMnO}_3$  previously obtained polycrystalline powder in a 7 : 1 ratio and annealed in a platinum crucible at 1250 °C for 48 h in oxygen. After that, the temperature was decreased down to 1000 °C at a rate of 0.5 °C  $\text{h}^{-1}$  and the flux was then decanted. The well-shaped hexagonal platelike  $ab$  face of typical size  $3 \times 5 \times 0.2$  mm<sup>3</sup> was removed from the bottom of crucible. A Bruker Instrument Model 113 Fourier Transform Spectrometer, equipped with a mercury light source and a composite Si bolometer, was used to collect and analyze spectra with a resolution of 0.5  $\text{cm}^{-1}$ . For measurements under a high magnetic field up to 9 T the samples were placed in the

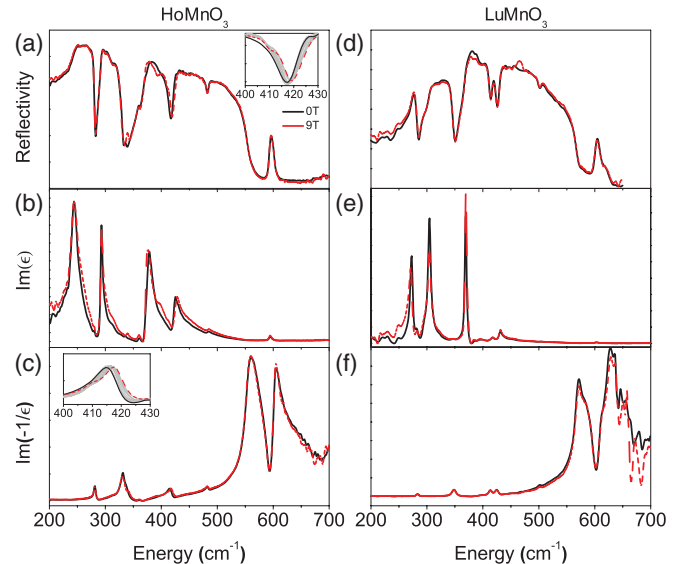


FIG. 2. (Color online) Far-infrared reflectance ( $E \perp c$ ) at 4.2 K, imaginary part of the dielectric function  $\text{Im}(\epsilon)$ , and loss function  $\text{Im}(-1/\epsilon)$  for  $\text{HoMnO}_3$  (a, b, and c) and  $\text{LuMnO}_3$  (d, e, and f). The insets show frequency shifts of  $\text{HoMnO}_3$  reflectance (a) and LO frequency (c) induced by applied magnetic fields (not observed in  $\text{LuMnO}_3$ ).

bore of a superconducting magnet positioned in a helium bath cryostat at 4.2 K.

## III. DISCUSSION

### A. Phonon assignment

$E1$  phonons are detected in our experimental configuration ( $E \perp c$ ). Figures 2(a) and 2(d) show the optical reflectance of  $\text{HoMnO}_3$  and  $\text{LuMnO}_3$  at 4.2 K. Optical transverse (TO) and longitudinal (LO) mode energies and their corresponding atomic displacements are determined (Table I). They correspond to peak positions in the imaginary parts of the dielectric functions  $\text{Im}(\epsilon)$  [Figs. 2(b) and 2(e)] and the loss functions  $\text{Im}(-1/\epsilon)$  [Figs. 2(c) and 2(f)], respectively. Superexchange between rare earth and manganese plays a major role in the hexagonal manganite multiferroic character.<sup>8,13,14</sup> This has been particularly observed by Hur *et al.*<sup>3</sup> below  $T_{\text{Ho}}$ , where an enhancement of the electric polarization occurs at the holmium magnetic transition from ferrimagnetic  $\text{Ho}_2$  and  $\text{Ho}_1$  to antiferromagnetic ordering of  $\text{Ho}_2$ . Also, when the

TABLE I.  $E1$  Far-infrared active mode frequencies ( $\text{cm}^{-1}$ ) in  $\text{HoMnO}_3$  and  $\text{LuMnO}_3$ .

Direction of the largest atomic displacements <sup>10</sup>	$\text{HoMnO}_3$ TO/LO	$\text{LuMnO}_3$ TO/LO
$a, b$ (Ho, Lu)	164.8/165.7	
$a, b$ ( $O_B$ ) + $a, c$ ( $O_A$ ); $c$ (Mn)	243.3/281.5	275.5/282.9
$a, b$ ( $O_A$ ) - $a, b$ ( $O_B$ )	292.3/331.7	307.9/348.1
$a, b$ ( $O_A$ )	374.1/415.5	371.5/413.3
$a, b$ ( $O_B$ ) - $a, b$ ( $O_A$ , Mn)	424.0/482.1	430.8/500.9
$a, b$ ( $O_B, O_A$ ) - $a, b$ (Mn)	484.1/562.2	502.8/570.9
$a, b$ ( $O_B$ )	595.3/606.5	602.8/628.1

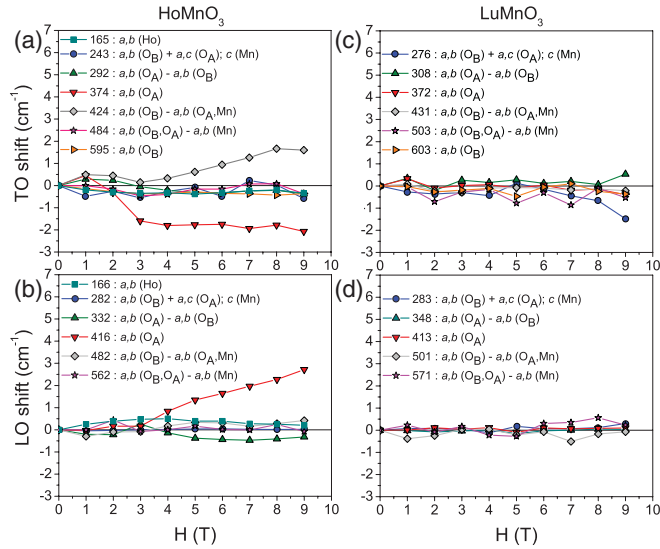


FIG. 3. (Color online) Frequency evolutions of TO and LO phonons in HoMnO<sub>3</sub> (a and b) and LuMnO<sub>3</sub> (c and d) as a function of the magnetic field. O<sub>A</sub> and O<sub>B</sub> correspond to apical and basal oxygen, respectively.

magnetic field is applied below  $T_{\text{Ho}}$ , the electric polarization is remarkably reinforced. In our experiment, interplane exchange interaction can be indirectly monitored through phonon energy evolutions that are associated with rare-earth, manganese, and oxygen ions. In Figs. 3(a)–3(d), TO and LO phonon energy behaviors under the applied magnetic field are shown for HoMnO<sub>3</sub> and LuMnO<sub>3</sub>. While some HoMnO<sub>3</sub> phonons are shifted, those of LuMnO<sub>3</sub> remain unaffected by the applied magnetic field. This suggests an important role for the Ho<sup>3+</sup> magnetic moment in the process. The principal phonon affected by the magnetic field involves apical oxygen oscillations in the  $ab$  plane. Its TO mode (374 cm<sup>-1</sup>) softens by 2 cm<sup>-1</sup> and its LO mode (416 cm<sup>-1</sup>) hardens by 3 cm<sup>-1</sup>. The other TO mode that hardens by 2 cm<sup>-1</sup> corresponds to the stretching of the hexahedral oxygen cage at 424 cm<sup>-1</sup> in the  $ab$  plane. Remarkably, phonon energy shifts of the order of a few cm<sup>-1</sup> start at 2 T when manganese spins rotate in the  $ab$  plane, and the symmetry group of the spin frustration changes from  $P6_3cm$  to  $P6_3c'm'$ .<sup>3,23</sup> Such magnitude of mode energy shift is indicative of a renormalization of the hybridization and superexchange interaction under the applied magnetic field that excludes atomic displacements. Actually, to reproduce the measured polarization at 5 T exclusively by atomic displacements, the latter should be of the order of 10<sup>-4</sup> Å and would result in only a 10<sup>-2</sup> cm<sup>-1</sup> phonon shift.

### B. Effective charges

The Born effective charge  $Z_k^*$  refers to the change of polarization that would be observed under the condition of zero macroscopic electric field.<sup>11,24</sup> It involves both static and dynamic contributions to the electric dipole moment. For simple materials with purely ionic character such as binary crystals and simple semiconductors, the Born effective charge value corresponds to the nominal ionic charges. However, it could deviate remarkably in the ferroelectrics (e.g., in BaTiO<sub>3</sub>,  $Z_{\text{Ti}}^* = 7.25$  and  $Z_{\text{O}}^* = -5.71$  based on first principal calcula-

tions) and it succeeds to predict correctly the spontaneous polarization.<sup>24</sup> The Born effective charge can be written in terms of the TO and LO optical frequencies,<sup>25</sup> Eq. (1):

$$\frac{4\pi}{v_c} \sum_{k=1}^n \frac{Z_k^{*2}}{m_k} = 4\pi^2 \sum_{j=1}^N (\omega_{\text{LO}j}^2 - \omega_{\text{TO}j}^2), \quad (1)$$

where  $v_c$  is the unit cell volume,  $j$  denotes the phonon mode, and  $m_k$  is the mass of the atom  $k$ . The electric neutrality of the system is respected with the relation  $\sum_k Z_k^* = 0$ . Considering that the electric charge of the rare earth ( $Z_{\text{Ho}}^*$ ) and manganese ( $Z_{\text{Mn}}^*$ ) are equal,<sup>11</sup> we write

$$\begin{aligned} \sum_{k=1}^n \frac{Z_k^{*2}}{m_k} &= Z \left[ n_{\text{Ho}} \frac{(Z_{\text{Ho}}^*)^2}{m_{\text{Ho}}} + n_{\text{Mn}} \frac{(Z_{\text{Mn}}^*)^2}{m_{\text{Mn}}} + n_{\text{O}} \frac{(Z_{\text{O}}^*)^2}{m_{\text{O}}} \right] \\ &= \underbrace{\left[ \frac{27/2}{m_{\text{Ho}}} + \frac{27/2}{m_{\text{Mn}}} + \frac{18}{m_{\text{O}}} \right]}_{\frac{v_c}{4\pi} \mu} (Z_{\text{O}}^*)^2. \end{aligned} \quad (2)$$

Fitting the reflectivity spectra with Drude-Lorentz oscillators<sup>11</sup> we have calculated  $Z_k^*$  ( $-2.3$  and  $3.5$  for the O and Ho, respectively). These results are similar to those found in YMnO<sub>3</sub> and LuMnO<sub>3</sub> in the same configuration ( $E \perp c$ ) at 300 K, while measurements in the  $E \parallel c$  configuration indicate important charge anisotropies.<sup>11,22</sup> These values are also consistent with the effective charges obtained for YMnO<sub>3</sub> from first-principle calculations ( $Z_{\text{Y}}^* = 3.6$ ,  $Z_{\text{Mn}}^* = 3.3$ ,  $Z_{\text{O}_{\text{apical}}}^* = -2.3$ , and  $Z_{\text{O}_{\text{basal}}}^* = -2.2$ ).<sup>26</sup> It is noteworthy that deviations from the nominal values ( $-2$  and  $3$ ) are small in hexagonal manganites compared to common ferroelectric materials such as BaTiO<sub>3</sub>, SrTiO<sub>3</sub>, and WO<sub>3</sub>, where  $Z_{\text{W}}^*$  is the double of the nominal charge.<sup>24,27</sup> Being interested in the variation of the effective charge we calculate  $\delta Z_{\text{O}}^*$  which is induced by a magnetic field according to

$$\begin{aligned} (Z_0^* + \delta Z^*)^2 &= \frac{4\pi^2}{\mu} \sum_{j=1}^N [(\omega_{\text{LO}j} + \delta\omega_{\text{LO}j})^2 - (\omega_{\text{TO}j} + \delta\omega_{\text{TO}j})^2], \\ \delta Z^* &= \frac{4\pi^2}{\mu Z_0^*} \sum_{j=1}^N (\omega_{\text{LO}j} \delta\omega_{\text{LO}j} - \omega_{\text{TO}j} \delta\omega_{\text{TO}j}), \end{aligned} \quad (3)$$

and we obtain  $\sim 2.5 \times 10^{-3}$  at 5 T. With the electric neutrality relation, we can also calculate  $\delta Z_{\text{Ho}}^*$  and  $\delta Z_{\text{Mn}}^*$  ( $\sim 3.8 \times 10^{-3}$  at 5 T). Using the  $\delta Z_k^*$  values we calculate the bulk polarization variation as a function of the applied magnetic field in a unit cell corresponding to HoMnO<sub>3</sub> crystallographic parameters as obtained from neutron diffraction. We also correlate the Ho<sub>1</sub> and Ho<sub>2</sub> relative  $c$  shifts with the measured polarization<sup>3</sup> [eq. (4)],

$$P(H) - P(H=0) = \frac{1}{v_c} \sum_k \delta Z_k^*(H). \quad (4)$$

Compared with the experimental measurements of Hur *et al.*,<sup>3</sup> the prediction is quite satisfactory (Fig. 4). Actually,  $\delta P$  changes smoothly around 2 T to reach a magnitude of  $\sim 70 \mu\text{C m}^{-2}$  at 5 T. This suggests that the external magnetic field induces a partial electronic charge transfer between Ho<sup>3+</sup>

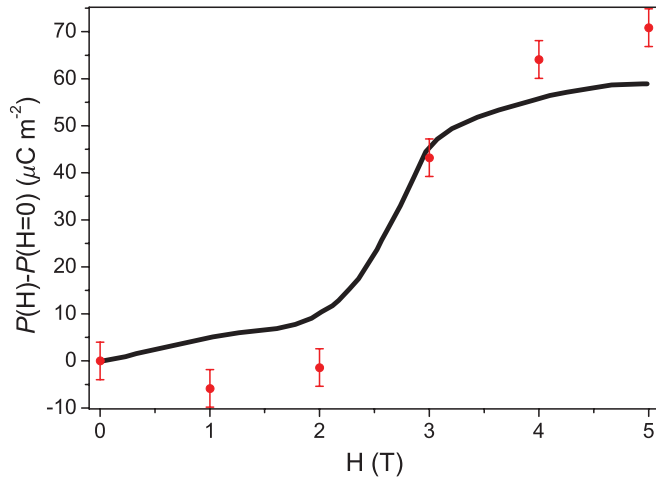


FIG. 4. (Color online) Magnetic dependence of the induced electric polarization as measured by Hur *et al.*<sup>3</sup> (black line) and as predicted by our measurements at 4.2 K in HoMnO<sub>3</sub> (red circles).

and O<sup>2-</sup> ions that raises the ferroelectricity and affects the Ho-Mn superexchange. The apical oxygen is involved in the hybridization process since its mode frequencies TO and LO are most affected by the magnetic field. In LuMnO<sub>3</sub> where the rare-earth spin is absent the magnetoelectric phenomenon is not expected as confirmed by the absence of apical oxygen phonon shifts under the applied magnetic field.

#### IV. CONCLUSION

HoMnO<sub>3</sub> and LuMnO<sub>3</sub> single crystal magnetoinfrared reflectances have been performed at 4.2 K ( $T < T_{HO}$ ) as a function of the applied magnetic field up to 9 T. Apical oxygen phonon energy shifts are observed in HoMnO<sub>3</sub> but are absent in LuMnO<sub>3</sub>, which indicates the importance of the Ho<sup>3+</sup> magnetic moment and the superexchange mechanism in the magnetoelectric process. The Born effective charges as a function of the magnetic field have been calculated from the phonon energy shifts allowing us to predict straightforwardly, with no adjustable parameters, the low temperature electric polarization change as measured in HoMnO<sub>3</sub> by Hur *et al.*<sup>3</sup> In contrast to previous studies that imply basal oxygen hybridizations to explain ferroelectricity,<sup>11,16-20</sup> our study underlines the role of the apical oxygens in the applied magnetic field modulated hybridization and corresponding charge transfer. Interestingly, despite the strong magnetoelectric effect in the RMn<sub>2</sub>O<sub>5</sub> family,<sup>28</sup> ~10 times more than in the hexagonal RMnO<sub>3</sub>,<sup>3</sup> a magnetic field of 18 T was needed to shift the phonon frequencies by 2 cm<sup>-1</sup> in DyMn<sub>2</sub>O<sub>5</sub><sup>29</sup> while we detected with 9 T a relatively important phonon frequency shift of 3 cm<sup>-1</sup> in HoMnO<sub>3</sub>. This underlines, in addition to possible magnetostriction, a major difference in the magnetoelectric mechanisms of these two manganite families, a crystalline distortion in the case of DyMn<sub>2</sub>O<sub>5</sub> as compared to a hybridization and a charge transfer in HoMnO<sub>3</sub>.

<sup>1</sup>J. F. Scott, *Nat. Mater.* **6**, 256 (2007).

<sup>2</sup>T. Lottermoser, T. Lonkai, U. Amann, D. Hohlwein, J. Ihringer, and M. Fiebig, *Nature (London)* **430**, 541 (2004).

<sup>3</sup>N. Hur, I. K. Jeong, M. F. Hundley, S. B. Kim, and S.-W. Cheong, *Phys. Rev. B* **79**, 134120 (2009).

<sup>4</sup>D. Khomskii, *Physics* **2**, 20 (2009).

<sup>5</sup>S. Lee, A. Pirogov, M. Kang, K.-H. Jang, M. Yonemura, T. Kamiyama, S.-W. Cheong, F. Gozzo, N. Shin, H. Kimura, Y. Noda, and J.-G. Park, *Nature (London)* **451**, 805 (2008).

<sup>6</sup>N. Iwata and K. Kohn, *J. Phys. Soc. Jpn.* **67**, 3318 (1998).

<sup>7</sup>J. Vermette, S. Jandl, and M. M. Gospodinov, *J. Phys. Condens. Matter* **20**, 425219 (2008).

<sup>8</sup>J. Vermette, S. Jandl, A. A. Mukhin, V. Y. Ivanov, A. Balbashov, M. M. Gospodinov, and L. Pinsard-Gaudart, *J. Phys. Condens. Matter* **22**, 356002 (2010).

<sup>9</sup>M. N. Iliev, H.-G. Lee, V. N. Popov, M. V. Abrashev, A. Hamed, R. L. Meng, and C. W. Chu, *Phys. Rev. B* **56**, 2488 (1997).

<sup>10</sup>A. P. Litvinchuk, M. N. Iliev, V. N. Popov, and M. M. Gospodinov, *J. Phys. Condens. Matter* **16**, 809 (2004).

<sup>11</sup>M. Zaghrioui, V. Ta Phuoc, R. A. Souza, and M. Gervais, *Phys. Rev. B* **78**, 184305 (2008).

<sup>12</sup>D. Lee, A. Yoon, S. Y. Jang, J.-G. Yoon, J.-S. Chung, M. Kim, J. F. Scott, and T. W. Noh, *Phys. Rev. Lett.* **107**, 057602 (2011).

<sup>13</sup>M. Fiebig, C. Degenhardt, and R. V. Pisarev, *Phys. Rev. Lett.* **88**, 027203 (2001).

<sup>14</sup>M. Poirier, J. C. Lemyre, P.-O. Lahaie, L. Pinsard-Gaudart, and A. Revcolevschi, *Phys. Rev. B* **83**, 054418 (2011).

<sup>15</sup>A. K. Singh, S. Patnaik, S. D. Kaushik, and V. Siruguri, *Phys. Rev. B* **81**, 184406 (2010).

<sup>16</sup>D.-Y. Cho, J.-Y. Kim, B.-G. Park, K.-J. Rho, J.-H. Park, H.-J. Noh, B. J. Kim, S.-J. Oh, H.-M. Park, J.-S. Ahn, H. Ishibashi, S.-W. Cheong, J. H. Lee, P. Murugavel, T. W. Noh, A. Tanaka, and T. Jo, *Phys. Rev. Lett.* **98**, 217601 (2007).

<sup>17</sup>C. Zhong, Q. Jiang, H. Zhang, and X. Jiang, *Appl. Phys. Lett.* **94**, 224107 (2009).

<sup>18</sup>J. Kim, K. C. Cho, Y. M. Koo, K. P. Hong, and N. Shin, *Appl. Phys. Lett.* **95**, 132901 (2009).

<sup>19</sup>M.-A. Oak, J.-H. Lee, H. M. Jang, J. S. Goh, H. J. Choi, and J. F. Scott, *Phys. Rev. Lett.* **106**, 047601 (2011).

<sup>20</sup>M.-A. Oak, J.-H. Lee, and H. M. Jang, *Phys. Rev. B* **84**, 153106 (2011).

<sup>21</sup>M. Fiebig, D. Fröhlich, K. Kohn, S. Leute, T. Lottermoser, V. V. Pavlov, and R. V. Pisarev, *Phys. Rev. Lett.* **84**, 5620 (2000).

<sup>22</sup>A. B. Souchkov, J. R. Simpson, M. Quijada, H. Ishibashi, N. Hur, J. S. Ahn, S. W. Cheong, A. J. Millis, and H. D. Drew, *Phys. Rev. Lett.* **91**, 027203 (2003).

<sup>23</sup>M. Fiebig, T. Lottermoser, and R. Pisarev, *J. Appl. Phys.* **93**, 8194 (2003).

<sup>24</sup>P. Ghosez, J.-P. Michenaud, and X. Gonze, *Phys. Rev. B* **58**, 6224 (1998).

<sup>25</sup>K. Tochi, T. Ohgaku, and N. Takeuchi, *J. Mater. Sci. Lett.* **8**, 1331 (1989).

<sup>26</sup>B. B. Van Aken, T. T. Palstra, A. Filippetti, and N. A. Spaldin, *Nature (London)* **3**, 164 (2004).

<sup>27</sup>F. Detraux, P. Ghosez, and X. Gonze, *Phys. Rev. B* **56**, 983 (1997).

<sup>28</sup>S.-W. Cheong and M. Mostovoy, *Nat. Mater.* **6**, 13 (2007).

<sup>29</sup>J. Cao, L. I. Vergara, J. L. Musfeldt, A. P. Litvinchuk, Y. J. Wang, S. Park, and S.-W. Cheong, *Phys. Rev. Lett.* **100**, 177205 (2008).